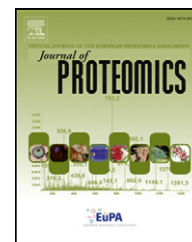


Available online at www.sciencedirect.com

SciVerse ScienceDirect

www.elsevier.com/locate/jprot

Proteomic investigation of the interactome of FMNL1 in hematopoietic cells unveils a role in calcium-dependent membrane plasticity

Yanan Han^{a, b}, Guangchuang Yu^b, Hakan Sarioglu^c, Amélia Caballero-Martinez^a, Fabian Schlott^a, Marius Ueffing^{c, d}, Hannelore Haase^e, Christian Peschel^a, Angela M. Krackhardt^{a, f, *}

^aMedizinische Klinik III, Klinikum rechts der Isar, Technische Universität München, Ismaninger Str. 22, 81675 Munich, Germany

^bInstitute of Life and Health Engineering, Jinan University, Guangzhou 510632, PR China

^cDepartment of Protein Sciences, Helmholtz Zentrum München, German Research Center for Environmental Health, Ingolstädter Landstr. 1, 85764 Neuherberg, Germany

^dDivision of Experimental Ophthalmology and Medical Proteome Center, Center of Ophthalmology, University of Tübingen, Tübingen, Germany

^eMax-Delbrück-Centrum für Molekulare Medizin Berlin-Buch, Forschungsgruppe Molekulare Muskelphysiologie, Robert-Rössle-Str. 10, 13092 Berlin, Germany

^fClinical Cooperation Group Antigen-specific Immunotherapy, Helmholtz Zentrum München, German Research Center for Environmental Health, Neuherberg and Technical University Munich, Klinikum rechts der Isar, Munich, Germany

ARTICLE INFO

Article history:

Received 28 September 2012

Accepted 18 November 2012

Keywords:

FMNL1

AHNAK1

Membrane plasticity

ABSTRACT

Formin-like 1 (FMNL1) is a formin-related protein highly expressed in hematopoietic cells and overexpressed in leukemias as well as diverse transformed cell lines. It has been described to play a role in diverse functions of hematopoietic cells such as phagocytosis of macrophage as well as polarization and cytotoxicity of T cells. However, the specific role of FMNL1 in these processes has not been clarified yet and regulation by interaction partners in primary hematopoietic cells has never been investigated. We performed a proteomic screen for investigation of the interactome of FMNL1 in primary hematopoietic cells resulting in the identification of a number of interaction partners. Bioinformatic analysis considering semantic similarity suggested the giant protein AHNAK1 to be an essential interaction partner of FMNL1. We confirmed AHNAK1 as a general binding partner for FMNL1 in diverse hematopoietic cells and demonstrate that the N-terminal part of FMNL1 binds to the C-terminus of AHNAK1. Moreover, we show that the constitutively activated form of FMNL1 (FMNL1 γ) induces localization of AHNAK1 to the cell membrane. Finally, we provide evidence that overexpression or knock down of FMNL1 has an impact on the capacitative calcium influx after ionomycin-mediated activation of diverse cell lines and primary cells.

© 2012 Published by Elsevier B.V.

Abbreviations: FMNL1, formin-like 1; PBMC, peripheral blood mononuclear cell; CLL, chronic lymphatic leukemia; GO, gene ontology; MF, molecular function; CC, cellular component.

* Corresponding author at: Medizinische Klinik III, Klinikum rechts der Isar, Technische Universität München, Ismaningerstr. 22, 81675 München, Germany. Tel.: +49 89 4140 4124; fax: +49 89 4140 4879.

E-mail address: angela.krackhardt@lrz.tu-muenchen.de (A.M. Krackhardt).

1874-3919/\$ – see front matter © 2012 Published by Elsevier B.V.

<http://dx.doi.org/10.1016/j.jprot.2012.11.015>

Please cite this article as: Han Y, et al, Proteomic investigation of the interactome of FMNL1 in hematopoietic cells unveils a role in calcium-dependent membrane p..., J Prot (2012), <http://dx.doi.org/10.1016/j.jprot.2012.11.015>

1. Introduction

Formins belong to a protein family represented by 15 different members in humans which are involved in actin-dependent key cellular processes as polarization, migration, vesicle trafficking and cytokinesis [1]. Formin-like 1 (FMNL1) is particularly expressed in hematopoietic cells as well as overexpressed in malignant cell lines. It is functionally involved in a number of diverse cell-type specific functions such as phagocytosis in macrophages, centrosome orientation and cytotoxicity as well as maintenance of the Golgi complex in T cells [2-5]. It is so far not well understood how these different processes are regulated and which interaction partners are involved. Previously, diverse Rho GTPases have been described to interact with and regulate FMNL1 as shown by direct interaction in pull down assays [4,6,7]. Direct pull down assays further identified FMNL1-specific interaction partners as Profilin 1 and Profilin 2 in FMNL1-transfected cell lines [4]. Large proteomic screens revealed FMNL1 as an interaction partner for several proteins, such as growth arrest-specific protein 7 (GAS7), PRPF40A, transcription elongation regulator 1 (TCERG1) [8] as well as X-ray repair cross-complementing protein 6 (XRCC6) [9]. However, interaction partners of human FMNL1 in primary hematopoietic cells have never been investigated so far. This, however, might be essential for a deeper understanding of the multifaceted role of this protein in hematopoietic cells.

We here applied a systematic proteomic interaction screen in order to identify direct interaction partners of FMNL1 within different human primary hematopoietic cell populations. We thereby identified a number of interaction partners and confirmed several by direct immunoprecipitation. The highest number of unique peptides, as found by mass spectrometry, was derived from the scaffold protein AHNAK1. Bioinformatics analysis additionally suggests that AHNAK1 is a crucial interaction partner of FMNL1. We confirm AHNAK1 as the interaction partner of FMNL1 in diverse hematopoietic cells and demonstrate specific binding of the N-terminal part of FMNL1 to the C-terminal part of AHNAK1. Moreover, we here demonstrate that membrane localization of AHNAK1 can be directly modulated by a splice variant of FMNL1 (FMNL1 γ). Finally, membrane localization of AHNAK1 has been previously demonstrated to be calcium-dependent [10-14] and we present evidence that FMNL1 is involved in the modulation of the capacitative calcium influx induced by ionomycin.

These data provide insights into the regulation of FMNL1 in primary hematopoietic cells and demonstrate that AHNAK1 is a common interaction partner of FMNL1 potentially conjointly involved in calcium-dependent membrane processes during excitative responses of hematopoietic cells.

2. Materials and methods

2.1. Cells and cell lines

Peripheral blood mononuclear cells (PBMC) from healthy donors and patients with chronic lymphatic leukemia (CLL) were collected with donors' informed consent following the

requirements of the local ethical board and the principles expressed in the Helsinki Declaration. Patients had diagnosis of CLL by morphology, flow cytometric analysis and cytogenetics. PBMC were obtained by density gradient centrifugation on Ficoll/Hypaque (Biochrom). PBMC subpopulations from healthy donors were isolated by negative or positive magnetic bead depletion (Invitrogen). K562 (ATCC CCL-243) and breast carcinoma cell line MDA-MB 231 (CLS) were used for adenoviral transduction of FMNL1 splice variants. HEK293T embryonal kidney cells (ATCC CRL-1573) were utilized for FMNL1 protein expression after transfection whereas 293A (Invitrogen) cells were used for production of adenoviral supernatant as previously described [15]. Peptide-pulsed T2 cells were used for T cell polarization [16,17]. Autologous EBV-B cell lines cultured with IL-4 on CD40L expressing feeder cells [17] were used for colocalization studies of FMNL1 and AHNAK1.

2.2. Antibodies

The following antibodies were used: N-terminal-specific rat anti-human FMNL1 antibody 8A8 and C-terminal-specific rat anti-human FMNL1 antibodies 6F2, 5A1, 5B12 and 5C9 [15,18], rat anti-mumps-hemagglutinin-specific monoclonal IgG antibody TQL, mouse anti-human GAPDH monoclonal IgG (Sigma-Aldrich), rabbit anti-human AHNAK1 polyclonal antibody [19] and mouse anti-human AHNAK1 monoclonal antibody (Abnova, clone 3G7), mouse anti-HIS antibody (Anaspec, 61250), polyclonal rabbit anti-human ARHGAP4 (ATLAS) and polyclonal rabbit anti-human anti-ARHGAP17 (Abcam), anti-CD8-FITC (V5T-HIT8a), goat anti-mouse immunoglobulin antibody (Jackson), goat anti-rabbit immunoglobulin antibody (Jackson), goat anti-rat immunoglobulin antibody (Jackson), Cy3-labeled goat anti-rat immunoglobulin antibody (Jackson) and Cy5-labeled goat anti-rabbit and anti-mouse immunoglobulin antibody (Jackson).

2.3. Immunoprecipitation

Activated T cells, B cells and CLL cells were pelleted and lysed in CHAPS buffer for 30 min on ice followed by incubation with Sepharose G beads for preclearing. Freshly prepared Sepharose G beads were washed and the FMNL1 N-terminal-specific antibody 8A8 using the IgG2c control TQL antibody or the FMNL1 C-terminal-specific antibodies 6F2, 5A1, 5B12 and 5C9 using IgG2b control anti-flag antibody were added followed by rotating for 1 h at 4 °C. Sepharose G beads were then washed and incubated with precleared protein lysate on the rotator for 3 h at 4 °C. Elution was performed and probes were forwarded for SDS-PAGE on two separate gels. One gel was used for immunoblotting to analyze the efficiency of immunoprecipitation of FMNL1 using the FMNL1-specific antibody 6F2. Silver staining was performed with the other gel to visually detect specific immunoprecipitated bands. Samples from different IPs were subjected to in gel digestion by trypsin before MS analysis. The different IP samples have been analyzed reduced and alkylated as well as non-reduced.

2.4. LC-MS/MS analysis

Digested peptides were analyzed by nano-HPLC (Ultimate 3000, Dionex) coupled to a linear quadrupole ion trap-Orbitrap (LTQ

Orbitrap XL) mass spectrometer (Thermo Fisher) equipped with a nano-ESI source. A nonlinear gradient using 2% ACN in 0.1% formic acid in water and 0.1% formic acid in 98% acrylonitrile was used with a flow rate of 250 nl/min. The mass spectrometer was operated in the data-dependent mode to automatically switch between Orbitrap-MS and LTQ-MS/MS. The method used allowed sequential isolation of the ten most intense ions depending on signal intensity for fragmentation on the linear ion trap. High resolution MS scans in the orbitrap and MS/MS scans in the linear ion trap were performed in parallel.

All MS/MS data were analyzed using MASCOT (Matrix Science) version: 2.2.06 searched the human uniref 100 (version from 19.04.2011 (126,233 protein entries for *Homo sapiens*)) and NCBI databases (version from 15.05.2011 (237,237 protein entries for *Homo sapiens*)) assuming the digestion enzyme trypsin, including a fragment ion mass tolerance of 0.8 Da and a parent ion tolerance of 10 PPM. Iodoacetamide derivative of cysteine as stable and oxidation of methionine, deamidation of arginine and glutamine was specified in MASCOT as variable modifications. Scaffold (version Scaffold_2_02_03, Proteome Software) was used to validate MS/MS-based peptide and protein identifications. Protein identifications were accepted if they could be established at greater than 95.0% probability and contained at least 2 unique peptides.

2.5. Bioinformatics analysis

Gene Ontology (GO) enrichment analysis was adopted to uncover the common biological processes played by the interaction partners of FMNL1 in different cell types, with $p < 0.05$. A hypergeometric model was implemented to assess whether the number of selected genes associated with the GO term was at a frequency greater than expected by chance. Q-values [20] were estimated to control the false discovery rate (FDR) for multiple hypotheses testing, with q -value < 0.05 . These analyses were calculated by Bioconductor package clusterProfiler [21]. The analysis result contained some redundant biological processes, since the GO categories to which genes are assigned are not independent. To solve this issue, semantic similarity [22] among GO categories was used to aggregate closely related categories. The final result was visualized by clusterProfiler [21].

Based on the semantic similarities of GO terms used for gene annotation, we rank the protein inside the interactome by the average functional similarities between the protein and its interaction partners. GO semantic similarity, which has been verified in terms of the correlation with gene expression profiles [23], provides the basic for functional comparison of gene product, and thus has been widely applied in bioinformatics, such as protein-protein interaction analysis [24], pathway analysis [25] and gene function prediction [26]. Here, we measure the functional similarity among proteins. Functional similarity, which is defined as the geometric mean of their semantic similarities in molecular function (MF) and cellular component (CC) aspect of GO, is designed for measuring the strength of the relationship between each protein and its partners by considering function and location of proteins. Semantic similarities among interactome proteins in MF and CC were measured through the GOSemSim package

[22] using the Wang method which performs in a more accurate and unbiased manner by taking the GO topological structure into account [27]. Functional similarities were further estimated by the geometric mean of semantic similarities in MF and CC. The distributions of functional similarities were demonstrated in Fig. 1. Proteins, which have strong relationship in function and location among the proteins within the interactome, were essential for the interactome to exert their functions. Here, we used the average of functional similarities to rank protein in the FMNL1 interactome. A cutoff value of 0.75 was chosen.

2.6. T cell polarization assay

T2 cells were pulsed with the tyrosinase-derived peptide YMNGTMSQV as previously described [16,18]. T cells that retrovirally transduced with the tyrosinase-specific T cell clone IVSB [28] were co-incubated with T2 cells pulsed with the relevant peptide for 15 min and then processed for immunofluorescence staining as previously described [15].

2.7. Constructs and protein expression

DNA of different FMNL1 splice variants, FMNL1 Δ DAD and the G2TA4T mutant variant for adenoviral transduction were produced as previously described [15]. Adenovirally transduced

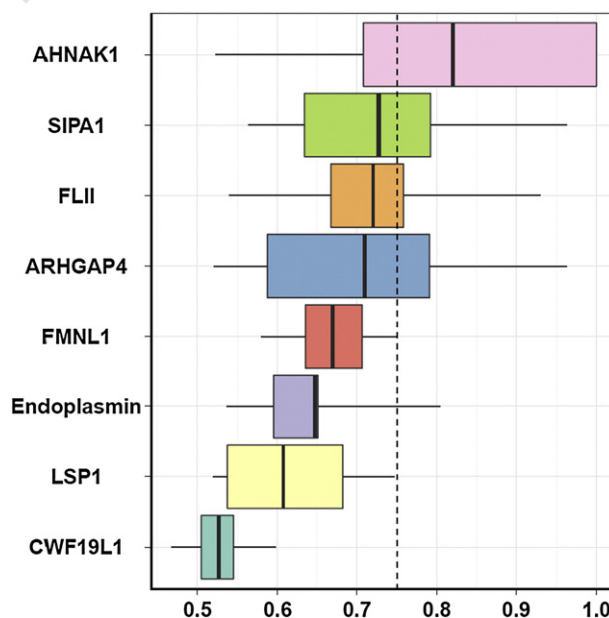


Fig. 1 – Summary of functional similarities of the FMNL1 interactome in T cells. The distributions of functional similarities were summarized as boxplots. The boxes represent the middle 50% of the similarities; the upper and lower boundaries show the 75th and 25th percentile. The lines in the boxes indicate the mean of the functional similarities. Proteins with a higher average functional similarity (cutoff > 0.75) were defined as party proteins, which are considered as the central proteins within the FMNL1 interactome in T cells. The dashed line represents the cutoff value.

238 cells were then used for confocal microscopy and calcium
239 signaling experiments.

240 Constructs with truncated and complete FMNL1 (Fig. 2B)
241 were cloned into a eukaryotic pCMV-His-tagged expression
242 vector (Invitrogen). T293 cells were transfected with the
243 plasmid of interests by calcium phosphate transfection. T293
244 cells were lysed with CHAPS lysis buffer and supernatant of
245 lysed cells was used for pull down assay.

246 C-terminal GST-tagged AHNAK1 constructs cloned into
247 pGEX-4T1 (C1, C2 and R4) have been previously described
248 [29]. BL-21-Codon Plus (DE3)-RIL bacteria (Stratagene) were
249 transformed with GST-tagged AHNAK1 constructs. Protein
250 expression was induced by IPTG (Sigma-Aldrich) incubation
251 for 2 h. Bacteria were collected by centrifugation and lysed with
252 NETN lysis buffer followed by sonification and centrifugation.
253 Supernatant was removed and used for pull down assay.

254 2.8. Immunofluorescence

255 Non-adherent cells were dropped on poly-L-lysine-coated cov-
256 erslips. Cells were fixed in 3% paraformaldehyde and then
257 washed, blocked with 10% FCS and stained with specific primary
258 and secondary antibodies as indicated. DAPI (Invitrogen) was
259 used for nuclear staining. Glass coverslips were mounted on the
260 cells in Mounting Medium (Vector Laboratories) and investigat-
261 ed by Confocal microscopy (Leica).

262 2.9. Pull-down assay

263 Bacterial supernatant containing GST-tagged AHNAK1 con-
264 structs was incubated with GST-Sepharose 4B beads (GE
265 Healthcare) rotating for 60 min at 4 °C. Beads were washed
266 intensively and proteins were verified by Coomassie simple
267 blue staining as well as immunoblot. Supernatant derived from
268 lysed 293T cells transfected with different FMNL1 constructs
269 was equilibrated with GST-Sepharose beads containing GST-
270 tagged AHNAK1 constructs rotating for 2 h at 4 °C. After
271 washing, elution was performed with 1×LDS+DTT and probes
272 were further analyzed by SDS-PAGE and western blot analysis.

273 2.10. siRNA knock down

274 Several FMNL1-specific siRNA were produced using the
275 Silencer siRNA Construction Kit (Applied Biosystems). The
276 best efficacy in down regulation of FMNL1 was reached with
277 the following sequences (MWG): 5'FMNL1 siRNA-AAAGGCG
278 TACCTGGACAATATCCTGTC and 3'FMNL1-AAATATTGTCCAG
279 GTAGCCCTCCTGTCTC. T cells stimulated with OKT3 and IL-2
280 were transfected by nucleofection using program T-20
281 (Amaxa Biosystems, Lonza). 4 h after transfection, cells were
282 collected, washed and cultured for 3 days prior to calcium
283 measurement and immunoblot.

284 2.11. Intracellular calcium measurement

285 Cells were transfected or transduced with different FMNL1
286 constructs. 2 days later, cells were harvested and adjusted to
287 10⁶/ml in pre-warmed medium in round bottom tubes.
288 Indo-1AM stain (Sigma-Aldrich) was added and cells were
289 then incubated for 30 min at 37 °C mixing every 10 min

during incubation. Stained cells were diluted to 0.1 Mio/ml
290 and kept in the dark until analysis. The free intracellular
291 calcium was analyzed by flow cytometry MoFlow (Dako)
292 recording the ratio of violet fluorescence (405 nm) and green
293 fluorescence (530 nm).
294

295 3. Results

296 3.1. Identification of interaction partners of FMNL1 in 297 primary hematopoietic cells by proteomic analysis 298

299 Since FMNL1 has been described to be predominantly expressed
300 in hematopoietic cells and involved in diverse cellular functions,
301 we wanted to identify novel key interaction partners of FMNL1
302 in primary hematopoietic cells including malignant cells
303 derived from patients with chronic lymphocytic leukemia
304 (CLL). We first focused on activated T cells and established IP
305 procedures for activated T cells using 5 FMNL1-specific anti-
306 bodies (N- and C-terminal). We then applied a proteomic
307 approach by immunoprecipitation of FMNL1 followed by
308 Nano-HPLC and LC-MS/MS analysis. As the N-terminal antibody
309 turned out to reveal the best results, this antibody has been
310 further applied for B cells and CLL cells. We thereby identified a
311 number of proteins, which were immunoprecipitated together
312 with FMNL1 but not with the control antibodies. In Table 1 and
313 Table S1-S4 best protein scores for a protein in all LC-MS/MS
314 approaches are shown. Table 1 shows the most abundant hits
315 also indicating the number of biological repeats for T cells and
316 all analyzed samples. The different IP samples have been
317 additionally analyzed reduced and alkylated and partially also
318 non-reduced further confirming actual results (data not shown).
319 We have identified a large number of novel interaction partners
320 which can be grouped into clusters involved in diverse
321 subcellular functions as proteins associated to the GTPase
322 signaling pathway (e.g. ARHGAP4, ARHGAP17, SIPA1, BTB/POZ
323 domain-containing adapter for CUL3-mediated RhoA degrada-
324 tion protein 3), scaffold proteins (e.g. AHNAK1, Plectin-1),
325 chaperons (e.g. Endoplasmic) and others. The biological pro-
326 cesses regulated by these interaction partners of FMNL1 were
327 further analyzed by clusterProfiler [21], which implemented a
328 hypergeometric model for identifying predominant biological
329 themes (Supplement, Fig. S1). The function of cytoskeleton
330 organization is over-represented across all the hematopoietic
331 cell types consistent with the fundamental role of the formin
332 defining FH2 domain in actin filament elongation [30]. Moreover,
333 the clusterProfiler analysis indicated a cell-type specific inter-
334 action pattern of the FMNL1 interactome suggesting that FMNL1
335 may display different functions in different cell types (Supple-
336 ment, Fig. S1).

337 In order to validate our data by other experimental
338 approaches we confirmed three interaction partners with
339 high numbers of identified unique peptides by direct immu-
340 noprecipitation. These experiments identified two of them,
341 AHNAK1 and ARHGAP4, as interaction partners of FMNL1 in
342 different probes derived from primary hematopoietic cells
343 (Fig. 2A, Supplement, Fig. S2A). In contrast, ARHGAP17 was
344 only identified as interaction partner of FMNL1 in B and CLL
345 cells (Supplement, Fig. S2B). We have also observed a number
346 of interaction candidates of FMNL1 identified only in CLL cells

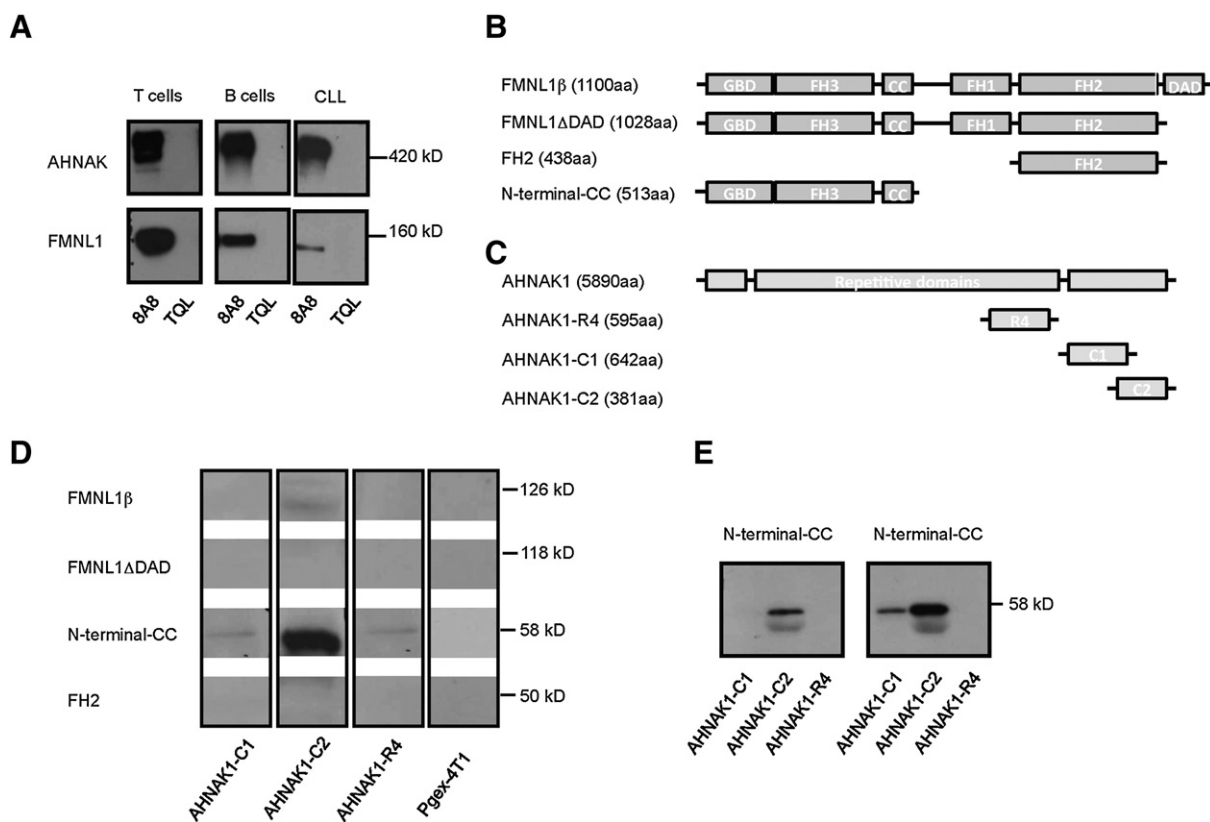


Fig. 2 – Co-immunoprecipitation of AHNAK1 and FMNL1 in T cells and identification of the interaction site. (A) FMNL1 was immunoprecipitated using the FMNL1-specific antibody 8A8. The TQL antibody served as isotype control. **Co-immunoprecipitation of AHNAK1 in T cells non-specifically stimulated with IL-2 and OKT3, B cells and CLL cells was confirmed by immunoblot. (B)** His-tagged constructs of FMNL1 cloned for pull down assays. **(C)** Scheme of AHNAK1 and cloned GST-tagged C-terminal AHNAK1 constructs R4, C1 and C2 used for pull-down assay. **(D and E)** Pull-down assays using GST-tagged AHNAK1 constructs and control GST. GST-tagged proteins were coupled to GST-Sepharose 4B and used in pull-down assays with His-tagged FMNL1 constructs. Proteins retained by defined AHNAK1 constructs were separated by SDS-PAGE and analyzed by immunoblotting with antibodies against HIS. Pull-down of the N-terminal-CC construct was demonstrated especially by AHNAK1 C2 (D and E) and in a single experiment also by AHNAK1-C1 (E).

347 (Table 1, Supplement, Table S3 and S4). One of them, Gemin5, 367
 348 was identified in both CLL samples. However, further analyses 368
 349 are necessary to segregate the interactome of FMNL1 in 369
 350 diverse hematopoietic and leukemic cells. 370

351 3.2. Evaluation of the interactome of FMNL1 I in T cells

352 In order to identify essential proteins of the FMNL1 interactome 371
 353 in T cells, we ranked proteins by their average functional 372
 354 similarity relationships among proteins within the interactome 373
 355 [31]. AHNAK1, SIPA1 and FLII were the three top-ranked proteins 374
 356 potentially playing central roles in the FMNL1 interactome in T 375
 357 cells. AHNAK1 was the only protein with a cutoff value >0.75 376
 358 (Fig. 1) which is widely used to separate significant and 377
 359 non-significant correlations [32,33]. However, FLII demonstrat- 378
 360 ing the average functional similarity score of 0.72 has been 379
 361 previously demonstrated to enhance actin assembly activity by 380
 362 directly binding to the formins DAAMI and mDia1 [34]. Thus our 381
 363 data suggest a similar role of FLII in its interaction with FMNL1. 382
 364 AHNAK1, which has not yet been previously identified as an 383
 365 interaction partner of FMNL1 or formins, has been previously 384
 366 reported to play an important role in T cell activation [35]. As 385

AHNAK1 has the highest average functional similarity in our 367
 analyses, we chose AHNAK1 for further functional investigation. 368

369 3.3. AHNAK1 interacts at its C-terminus with the N- 370 terminal region of FMNL1 371

AHNAK1 was consistently identified as an interaction partner of 371
 FMNL1 by mass spectrometry with a high number of unique 372
 peptides in T cells and other hematopoietic cells (Table 1, 373
 Supplement, Table S1 and data not shown). We further 374
 confirmed the interaction by co-immunoprecipitation experi- 375
 ments with FMNL1 in T cells and other hematopoietic cells 376
 (Fig. 2A). In order to localize the interaction site of FMNL1 with 377
 AHNAK1, we cloned different truncated His-tagged constructs of 378
 FMNL1 (Fig. 2B) and used previously described GST-tagged 379
 constructs of AHNAK1 (Fig. 2C and [29]) for pull down experi- 380
 ments. We were able to detect specific binding of the 381
 FMNL1-derived construct N-terminal-CC to the AHNAK1- 382
 derived C-terminal construct C2 (Fig. 2D) There was no specific 383
 interaction observed for the other constructs of FMNL1. Howev- 384
 er, one out of three experiments also demonstrated weak 385
 interaction with the AHNAK1-derived C-terminal construct C1 386

387 (Fig. 2E). These data demonstrate that AHNAK1 interacts at its
388 C-terminus with the N-terminal region of FMNL1.

389 3.4. Distinct patterns of FMNL1 and AHNAK1 localization 390 in primary T cells and K562 cells overexpressing diverse 391 FMNL1 splice variants

392 We investigated localizations of FMNL1 and AHNAK1 in
393 primary T cells as well as K562 cells transduced with different
394 splice variants of FMNL1. In non-specifically stimulated T
395 cells, we observed localization of FMNL1 in the cytoplasm
396 (Fig. 3A and B) as previously described [15]. In contrast,
397 AHNAK1 showed different patterns of localization, either in
398 the cytoplasm or at the cell membrane (Fig. 3A and B).
399 Quantification by counting demonstrated that AHNAK1 was
400 located intracellularly in most cases (Fig. 3C). Regarding
401 specifically stimulated T cells, AHNAK1 was polarized to the
402 immunological synapse (Fig. 3D and E). AHNAK1 partially
403 colocalized with FMNL1 at the immunological synapse
404 (Fig. 3D). We additionally overexpressed different splice
405 variants of FMNL1 in K562 cells. Wildtype K562 cells or K562
406 cells adenovirally transduced with GFP showed a mainly
407 intracellular distribution of FMNL1 and variable AHNAK1
408 localization (Fig. 4A, B). K562 cells transduced with diverse
409 FMNL1 splice variants showed a splice-variant dependent
410 localization of both FMNL1 and AHNAK1. Whereas K562 cells
411 transduced with FMNL1 α showed almost completely diver-
412 gent localization of FMNL1 and AHNAK1 (Fig. 4C), and

transduction with FMNL1 β resulted in colocalization of both 413
414 proteins mainly in the cytoplasm (Fig. 4D). In contrast, K562
415 cells adenovirally transduced with FMNL1 γ showed a clear
416 membranous localization of both, FMNL1 γ and AHNAK1
417 (Fig. 4E). Moreover, we could also detect co-localization of
418 FMNL1 γ and AHNAK1 in blebbing cells (Fig. 4F) [15].

3.5. FMNL1 enhances ionophore-mediated calcium influx 419

AHNAK1 is a scaffold protein, which plays an important role in 420
421 plasma membrane enlargement, exocytosis and repair
422 [11,12,36]. It has been previously reported that localization of
423 AHNAK1 is calcium-dependent and that ionophore-mediated
424 calcium influx induces AHNAK1 localization to the plasma
425 membrane [10–13]. Moreover, AHNAK1 has been shown to be
426 involved in calcium signaling and effector functions of T cells
427 [35,37]. Since transduction of K562 cells with FMNL1 γ induces
428 translocation of AHNAK1 to the cell membrane (Fig. 4E, F), we
429 hypothesized that FMNL1 may be also involved in calcium-
430 dependent membrane processes. Therefore, we aimed to
431 investigate if overexpression or down regulation of FMNL1
432 may affect ionophore-mediated calcium influx. We therefore
433 transduced MDA-MB-231 cells not expressing FMNL1 with
434 different splice variants and constructs of FMNL1 as previously
435 described [15]. Overexpression of FMNL1 in MDA-MB-231 cells
436 induced enhanced calcium influx after stimulation with
437 ionomycin as measured by Indo-1-AM-staining (Fig. 5A). Of
438 interest, transduction of FMNL1 α showed only a minor effect

t1.1 **Table 1 – Identification of potential interaction partners of FMNL1 by LC-MS/MS analysis in different hematopoietic cell**
t1.2 **populations.**

t1.3 t1.4	Eluted protein identified by mass spectrometry	Description	UniProt accession number	T cells ^a	Number of different biological samples in T cells	B cells ^a	CLL1 ^a	CLL2 ^a	Total number of different biological samples including T, B and CLL cells
t1.5	FMNL1	Formin-like 1	Q95466	25	5	47	56	29	8
t1.6	AHNAK1	AHNAK nucleoprotein	Q09666	40	4	273	311	286	7
t1.7	ARHGAP4	Rho GTPase activating protein 4	P98171	16	2	63	44	28	5
t1.8	CWF19L1	CWF19-like 1	Q69YN2	10	1	23	34	19	4
t1.9	PARP	Poly [ADP-ribose] polymerase 1	P09874	8	4	46	21	3	7
t1.10	Endoplasmic	Heat shock protein 90 kDa beta	P14625	2	3	19	3	3	6
t1.11	FLI1	Flightless-1 homolog	Q13045	3	3	–	–	–	3
t1.12	LSP-1	Lymphocyte-specific protein 1	P33241	2	4	–	–	–	4
t1.13	SIPA1	Signal-induced proliferation associated protein 1	Q96FS4	2	3	–	–	–	3
t1.14	ARHGAP17	Rho GTPase activating protein 17	Q68EM7	–	–	17	4	–	2
t1.15	PLTN	Plectin-1	Q15149	–	–	15	36	–	2
t1.16	TIA-1	Nucleolysin TIA-1 isoform p40	P31483	–	–	2	4	2	3
t1.17	hBACURD3	BTB/POZ domain-containing adapter for CUL3-mediated RhoA degradation protein 3	Q9H3F6	–	–	2	7	–	2
t1.18	Gemin 5	Gem-associated protein 5	Q8TEQ6	–	–	–	22	2	2
t1.19	^a Number of unique peptides identified.								

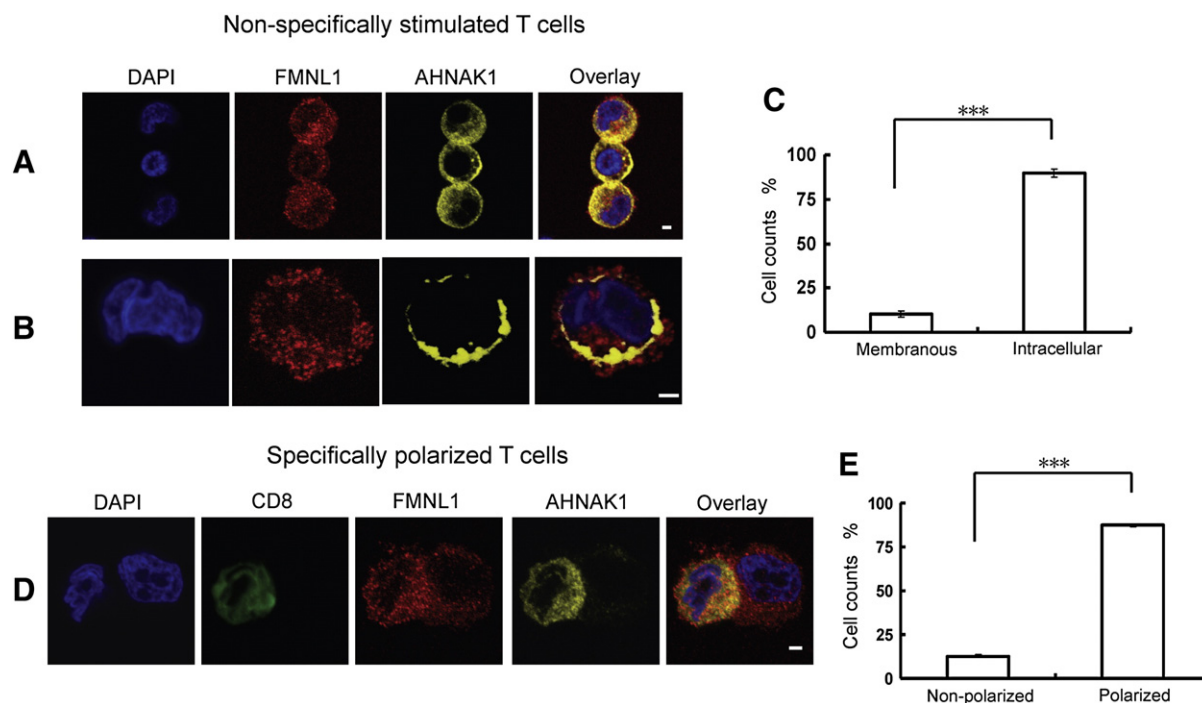


Fig. 3 – Immunofluorescence staining of AHNAK1 and FMNL1 shows diverse patterns in non-specifically and specifically stimulated T cells. (A, B) T cells non-specifically stimulated with IL-2 and OKT3 were stained with DAPI for nuclear staining (blue), rat anti-human FMNL1 6F2 followed by Cy3-labeled goat anti-rat antibody (red) and mouse anti-human AHNAK1 followed by Cy5-labeled goat anti-mouse antibody (yellow). Cells were analyzed at the confocal microscope, scale bar: 2 μ m. (C) Quantification of localization of AHNAK1 in non-specifically stimulated T cells. * indicates $p < 0.0001$ (D) The tyrosinase-specific T cell clone IVSB [28] was used for polarization assay and stimulated with T2 cells pulsed with the HLA-A2-binding tyrosinase-derived peptide 369 (YMNGTMSQV) for 15 min. Mixed cell populations were then fixed and stained with DAPI for nuclear staining (blue), mouse anti-human CD8 FITC (green), rat anti-human FMNL1 6F2 followed by Cy3-labeled goat anti-rat antibody (red) and mouse anti-human AHNAK1 followed by Cy5-labeled goat anti-mouse antibody (yellow). Cells were analyzed at the confocal microscope, scale bar: 2 μ m. (E) Quantification of polarization of AHNAK1 in specifically stimulated T cells. *** indicates $p < 0.0001$. Two sample t-tests were applied to calculate p value. (For interpretation of the references to color in this figure legend, the reader is referred to the web version of this article.)**

439 compared to the other splice variants including constitutively
 440 activated FMNL1 γ and FMNL1 Δ DAD. However, transduction of
 441 the G2TA4T construct containing a mutation of the N-terminal
 442 myristoylation site of FMNL1 showed no impact on calcium
 443 signaling (Fig. 5A), suggesting that modulation of calcium influx
 444 by FMNL1 is not necessarily associated with its membrane
 445 localization mediated by N-terminal myristoylation. A similar
 446 effect on calcium signaling of FMNL1 has also been observed in
 447 other cell lines as HEK293T cells and HT1080 cells transfected or
 448 adenovirally transduced with FMNL1 (Supplement, Fig. S3). We
 449 additionally investigated calcium influx of stimulated T cells by
 450 ionomycin after knock down of FMNL1 (Fig. 5B). In fact, calcium
 451 influx was reduced after knock down of FMNL1 when compared
 452 to the control siRNA (Fig. 5B).

453 4. Discussion

455 FMNL1 has been previously demonstrated to be involved in a
 456 number of different functional processes in diverse hematopoi-
 457 etic cell types as polarization and cytotoxicity of T cells [3] and
 458 phagocytosis as well as podosomal dynamics in macrophages

[4,6,38]. More recently, a role of FMNL1 in maintenance of
 459 structural integrity of the Golgi complex and lysosomes has
 460 been reported [5]. We performed a proteomic interaction screen
 461 in primary hematopoietic cells as activated T cells, B cells and
 462 CLL cells to identify novel interaction partners of FMNL1
 463 potentially providing further insights into the regulation and
 464 function of this multi-faceted protein.
 465

We thereby repeatedly identified a number of interaction
 466 proteins in diverse biological samples and technical repeats.
 467 Among these were several Rho GTPase modulating proteins
 468 as ARHGAP4 and ARHGAP17 which have been repeatedly
 469 identified with a significant number of unique peptides. Both
 470 proteins were verified by co-immunoprecipitation and direct
 471 immunoblot. ARHGAP4 belongs to the srGAP family and may
 472 bind to the proline-rich FH1 domain of FMNL1 by its SH3
 473 domain as previously reported for srGAP2 [7]. ARGHAP4 is
 474 highly expressed in embryonic neuronal tissue as well as
 475 hematopoietic cells [39,40]. It has been demonstrated to
 476 localize to the Golgi and microtubules and to mediate
 477 inhibition of axon outgrowth and cell motility [39,41]. Howev-
 478 er, ARHGAP4 activity may be dispensable for FMNL1 regula-
 479 tion as deletion of ARHGAP4 in patients with additional
 480

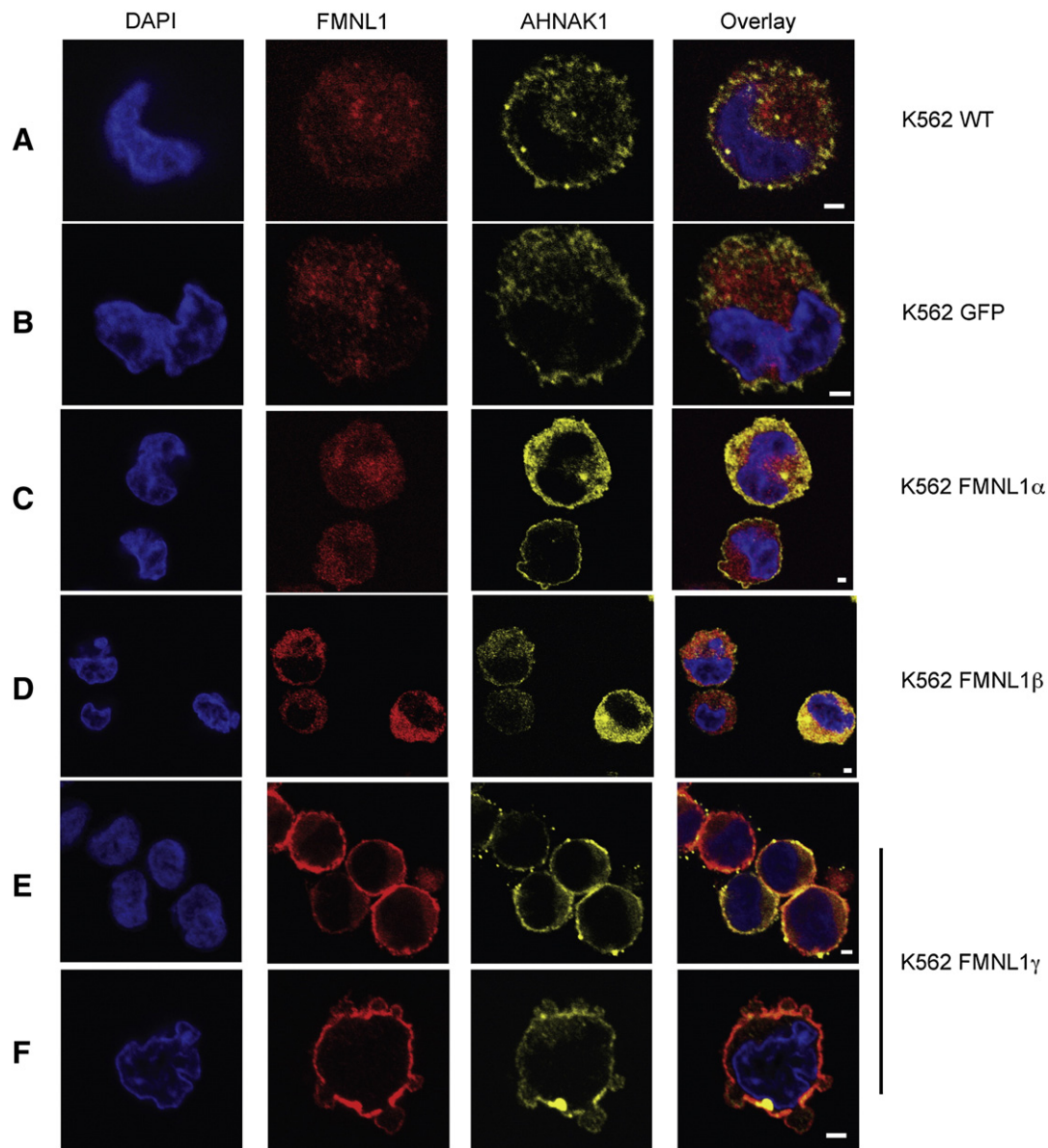


Fig. 4 – Colocalization of AHNAK1 and FMNL1 in K562 cells overexpressing different splice variants of FMNL1. K562 cells were adenovirally transduced with different FMNL1 splice variants as well as GFP control. Transduced cells and wildtype (WT) control were stained with DAPI for nuclear staining (blue), rat anti-human FMNL1 6F2 followed by Cy3-labeled goat anti-rat antibody (red) and mouse anti-human AHNAK1 followed by Cy5-labeled goat anti-mouse antibody (yellow). Cells were analyzed at the confocal microscope, scale bar: 2 μ m. (A) wildtype, (B) GFP, (C) FMNL1 α , (D) FMNL1 β , (E, F) FMNL1 γ . (For interpretation of the references to color in this figure legend, the reader is referred to the web version of this article.)

481 AVPR2 deletion and nephrogenic diabetes insipidus does not
 482 result in major perturbations of the immune system [40]. In
 483 contrast to ARHGAP4, ARHGAP17 (Rich1) has been identified
 484 as interaction partner of FMNL1 in B cells and one CLL cell
 485 sample but not in T cells suggesting a preferential cell-type
 486 specific regulation of FMNL1 by ARHGAP17 which was
 487 confirmed by western blot. The protein also belongs to the
 488 srGAP family containing a conserved N-terminal F-BAR
 489 domain, a central Rho-family GAP domain and a C-terminal
 490 SH3 domain. ARHGAP17 has been previously described to
 491 regulate Cdc42 and to be involved in organization of apical
 492 polarity in epithelial cells [42]. Moreover, ARHGAP17 is
 493 obviously involved in Rac1 regulation [43–45] and has been

suggested to play a role in inhibition of calcium-dependent
 exocytosis [43] as well as inhibition of Rac1 and the Ras-MAPK
 signaling pathways under growth suppressive conditions [45].

Bioinformatic analysis was performed and visualized by
 clusterProfiler in order to identify significant biological processes
 regulated by FMNL1 concentrating on proteins with enhanced
 statistical probability [46]. The analysis result suggested a
 cell-type specific interaction pattern. In order to further select
 proteins potentially significant in the FMNL1 interactome in T
 cells we applied further bioinformatics analyses by ranking
 through integration of protein semantic similarity [31,46].
 AHNAK1, SIPA1 and FLII were the three top-ranked proteins
 potentially playing central roles in the FMNL1 interactome in T

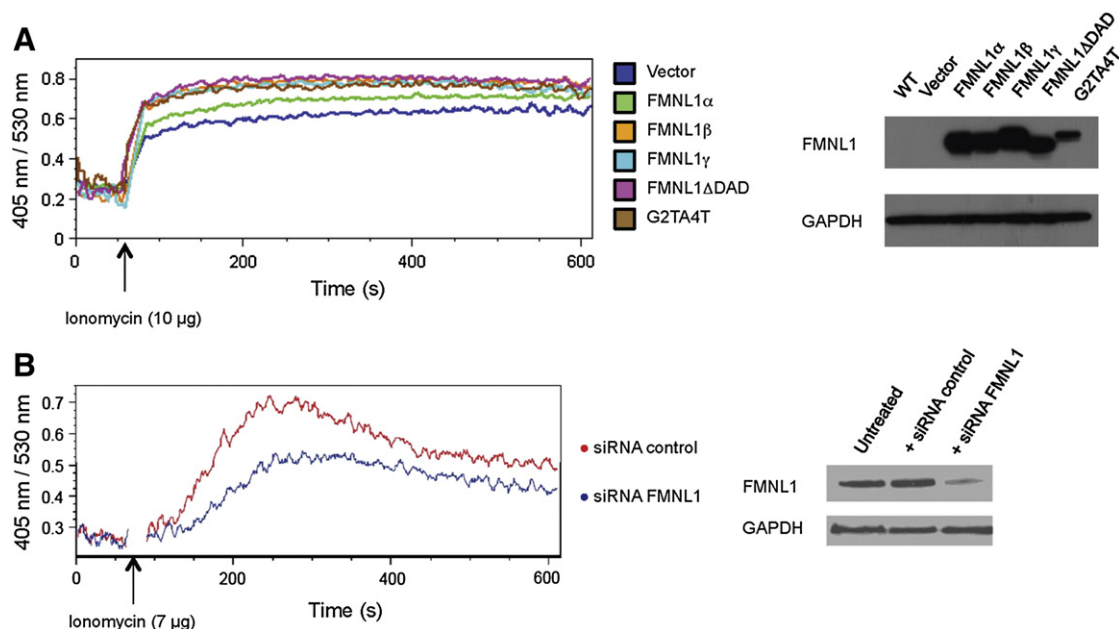


Fig. 5 – FMNL1 modulates ionophore-mediated calcium influx. (A) MDA-MB-231 cells were adenovirally transduced with different FMNL1 splice variants as well as the FMNL1 Δ DAD and G2TA4T mutant constructs. Cells were harvested and stained with Indo-1AM stain. Intracellular calcium was measured after stimulation of cells with ionomycin (10 μ g) and analyzed by flow cytometry recording the ratio of violet fluorescence (405 nm) and green fluorescence (530 nm) (left). Expression of FMNL1 constructs was verified by SDS-PAGE and immunoblot of cell lysates using the rat anti-human FMNL1-specific antibody 6F2 (right). One out of at least three independent experiments for MDA-MB-231 cells is shown. Two other experiments using different cell lines showed similar results (Fig. S3). (B) T cells non-specifically stimulated with IL-2 and OKT3 were transfected with an FMNL1-specific siRNA as well as a control siRNA by nucleofection. 3 days later, harvested cells were stimulated with ionomycin (7 μ g) and analyzed by flow cytometry recording the ratio of violet fluorescence (405 nm) and green fluorescence (530 nm) (left). Knock-down of FMNL1 was confirmed by SDS-PAGE and immunoblot of cell lysates using the rat anti-human FMNL1-specific antibody 6 F2 (right). One out of two independent experiments is shown. (For interpretation of the references to color in this figure legend, the reader is referred to the web version of this article.)

507 cells. FLII has been previously demonstrated to be a positive
508 regulator of Rho-induced linear actin assembly in Daam1 and
509 mDia1 [34]. Thus, our results suggest that FLII may be also a
510 positive regulator for actin polymerization for other formins as
511 FMNL1. AHNAK1 showed the highest functional similarity in our
512 analyses. This protein represents a scaffold protein involved in
513 different cellular processes such as calcium signaling in T cells
514 and cardiomyocytes [35,47,48] as well as membrane plasticity
515 and repair [11,12,36]. It has not been previously identified as an
516 interaction partner of FMNL1 or other formins. We confirmed
517 interaction of FMNL1 with AHNAK1 by co-immunoprecipitation
518 and subsequent immunoblot. We were further able to define
519 interaction sites of both proteins, as we observed specific binding
520 of the N-terminal construct of FMNL1 harboring also the
521 coiled-coil region to the C-terminal end of AHNAK1. The binding
522 localization of FMNL1 to the C-terminus of AHNAK1 is similar to
523 the previously reported interaction of AHNAK1 with diverse
524 proteins as Cav1.2 channel, actin, and the S100A10-annexin A2
525 complex [29,49]. It has been previously shown that the
526 C-terminal end of AHNAK1 is critically involved in subcellular
527 localization of AHNAK1 [13]. Moreover, structural analysis of the
528 S100A10-annexin A2-AHNAK1 complex recently suggested both
529 proteins to be involved in plasma membrane translocation of
530 AHNAK1 [49]. Apart from the similar interaction site we here
531 demonstrate that in K562 cells plasma membrane localization of

AHNAK1 to the cell membrane can be induced by overexpression
532 of FMNL1 γ but not the other FMNL1 splice variants. These data
533 indicate that especially FMNL1 γ may also be involved in
534 subcellular localization of AHNAK1 at the plasma membrane
535 and confirm that diverse splice variants of FMNL1 may harbor
536 distinct functions [5,15].
537

AHNAK has been previously repeatedly shown to be
538 involved in calcium-dependent membrane repair [11,36,50,51].
539 Subcellular localization of AHNAK1 has been demonstrated to
540 be calcium-dependent and AHNAK1 is located to the cell
541 membrane after capacitative calcium influx induced by
542 ionomycin [10–13]. In addition, AHNAK1 has been demonstrat-
543 ed to be involved in Cav1.1 channel regulation in T cells [35,37].
544 Thus, AHNAK1 seems to be regulated by calcium modulation
545 but also to represent a calcium modulator itself. By investiga-
546 tion of the impact of FMNL1 expression on the ionophore-
547 mediated calcium influx we have observed that overexpression
548 of FMNL1 in diverse cell lines results in enhanced capacitative
549 calcium influx after ionomycin treatment whereas FMNL1
550 knock down reduces calcium influx in primary T cells.
551 AHNAK1 itself might not be involved in ionomycin-mediated
552 calcium modulation as ionomycin-mediated calcium influx has
553 not been altered in AHNAK1 knock-out mice [35]. However,
554 calcium modulation of FMNL1 may further modulate the
555 activity of AHNAK1 and both proteins may interact in
556

557 calcium-dependent membrane processes [3,4,12,15,36]. The
 558 exact nature of calcium modulation by FMNL1 needs to be
 559 further investigated. Other identified interaction partners of
 560 FMNL1 as the voltage-dependent anion-selective channel
 561 protein 1 as well as chaperones as endoplasmic may be
 562 involved in calcium modulation induced by FMNL1 [52,53]. Of
 563 note, similar to FMNL1, AHNK1 has been also previously
 564 shown to be up-regulated in CLL cells [54]. Thus it will be
 565 important to further segregate the role of FMNL1, AHNK1 and
 566 interaction partners selectively identified in CLL samples as
 567 Gemin5 in healthy and malignant cells.

568 5. Conclusion

570 In conclusion, the proteomic screen of the interactome of
 571 FMNL1 provided novel information about general and cell-type
 572 specific interaction partners of FMNL1, demonstrated interac-
 573 tion of FMNL1 and AHNK1 as well as a splice-variant
 574 dependent close cooperation between AHNK1 and FMNL1 in
 575 modulation of membrane plasticity. Data point to a novel role of
 576 FMNL1 as modulator of capacitative calcium influx. Although
 577 these data need to be further confirmed they suggest that
 578 FMNL1 is involved in modulation of stimulation-associated
 579 calcium-dependent cytoskeletal membrane processes.

580 Acknowledgments

582 This work was funded by DFG KR2305/3-1 and China postdoc-
 583 toral science foundation 2011M501374.

584 Appendix A. Supplementary data

586 Supplementary data to this article can be found online at
 587 <http://dx.doi.org/10.1016/j.jprot.2012.11.015>.

588 REFERENCES

- 589 [1] Faix J, Grosse R. Staying in shape with formins. *Dev Cell*
 590 2006;10:693–706.
- 591 [2] Krackhardt AM, Witzens M, Harig S, Hodi FS, Zauls AJ,
 592 Chessia M, et al. Identification of tumor-associated antigens
 593 in chronic lymphocytic leukemia by SEREX. *Blood* 2002;100:
 594 2123–31.
- 595 [3] Gomez TS, Kumar K, Medeiros RB, Shimizu Y, Leibson PJ,
 596 Billadeau DD. Formins regulate the actin-related protein 2/3
 597 complex-independent polarization of the centrosome to the
 598 immunological synapse. *Immunity* 2007;26:177–90.
- 599 [4] Seth A, Otomo C, Rosen MK. Autoinhibition regulates cellular
 600 localization and actin assembly activity of the
 601 diaphanous-related formins FRLalpha and mDia1. *J Cell Biol*
 602 2006;174:701–13.
- 603 [5] Colon-Franco JM, Gomez TS, Billadeau DD. Dynamic
 604 remodeling of the actin cytoskeleton by FMNL1gamma is
 605 required for structural maintenance of the Golgi complex. *J*
 606 *Cell Sci* 2011;124:3118–26.
- 607 [6] Yayoshi-Yamamoto S, Taniuchi I, Watanabe T. FRL, a novel
 608 formin-related protein, binds to Rac and regulates cell
 609 motility and survival of macrophages. *Mol Cell Biol* 2000;20:
 610 6872–81.
- [7] Mason FM, Heimsath EG, Higgs HN, Soderling SH. Bi-modal
 612 regulation of a formin by srGAP2. *J Biol Chem* 2011;286:
 613 6577–86.
- [8] Ingham RJ, Colwill K, Howard C, Dettwiler S, Lim CS, Yu J,
 615 et al. WW domains provide a platform for the assembly of
 616 multiprotein networks. *Mol Cell Biol* 2005;25:7092–106.
- [9] Stelzl U, Worm U, Lalowski M, Haenig C, Brembeck FH,
 618 Goehler H, et al. A human protein–protein interaction
 619 network: a resource for annotating the proteome. *Cell*
 620 2005;122:957–68.
- [10] Hashimoto T, Gamou S, Shimizu N, Kitajima Y, Nishikawa T.
 622 Regulation of translocation of the desmoyokin/AHNK
 623 protein to the plasma membrane in keratinocytes by protein
 624 kinase C. *Exp Cell Res* 1995;217:258–66.
- [11] Cocucci E, Racchetti G, Podini P, Rupnik M, Meldolesi J.
 626 Enlargeosome, an exocytic vesicle resistant to nonionic
 627 detergents, undergoes endocytosis via a nonacidic route. *Mol*
 628 *Biol Cell* 2004;15:5356–68.
- [12] Cocucci E, Racchetti G, Podini P, Meldolesi J. Enlargeosome
 630 traffic: exocytosis triggered by various signals is followed by
 631 endocytosis, membrane shedding or both. *Traffic* 2007;8:
 632 742–57.
- [13] Nie Z, Ning W, Amagai M, Hashimoto T. C-terminus of
 634 desmoyokin/AHNK protein is responsible for its
 635 translocation between the nucleus and cytoplasm. *J Invest*
 636 *Dermatol* 2000;114:1044–9.
- [14] Benaud C, Gentil BJ, Assard N, Court M, Garin J, Delphin C,
 638 et al. AHNK interaction with the annexin 2/S100A10
 639 complex regulates cell membrane cytoarchitecture. *J Cell Biol*
 640 2004;164:133–44.
- [15] Han Y, Eppinger E, Schuster IG, Weigand LU, Liang X,
 642 Kremmer E, et al. Formin-like 1 (FMNL1) is regulated by
 643 N-terminal myristoylation and induces polarized membrane
 644 blebbing. *J Biol Chem* 2009;284:33409–17.
- [16] Liang X, Weigand LU, Schuster IG, Eppinger E, van der Griendt
 646 JC, Schub A, et al. A single TCR alpha-chain with dominant
 647 peptide recognition in the allorestricted HER2/neu-specific T
 648 cell repertoire. *J Immunol* 2010;184:1617–29.
- [17] Wiesner M, Zentz C, Mayr C, Wimmer R, Hammerschmidt W,
 650 Zeidler R, et al. Conditional immortalization of human B cells
 651 by CD40 ligation. *PLoS One* 2008;3:e1464.
- [18] Schuster IG, Busch DH, Eppinger E, Kremmer E, Milosevic S,
 653 Hennard C, et al. Allorestricted T cells with specificity for the
 654 FMNL1-derived peptide PP2 have potent antitumor activity
 655 against hematologic and other malignancies. *Blood* 2007;110:
 656 2931–9.
- [19] Haase H, Pagel I, Khalina Y, Zacharzowsky U, Person V,
 658 Lutsch G, et al. The carboxyl-terminal ahnak domain induces
 659 actin bundling and stabilizes muscle contraction. *FASEB J*
 660 2004;18:839–41.
- [20] Storey JD. A direct approach to false discovery rates. *J R Stat*
 662 *Soc Ser B (Stat Methodol)* 2002;64:479–98.
- [21] Yu G, He QY. Functional similarity analysis of human
 664 virus-encoded miRNAs. *J Clin Bioinforma* 2011;1:15.
- [22] Yu G, Li F, Qin Y, Bo X, Wu Y, Wang S. GOSemSim: an R
 666 package for measuring semantic similarity among GO terms
 667 and gene products. *Bioinformatics* 2010;26:976–8.
- [23] Sevilla JL, Segura V, Podhorski A, Guruceaga E, Mato JM,
 669 Martinez-Cruz LA, et al. Correlation between gene expression
 670 and GO semantic similarity. *IEEE/ACM Trans Comput Biol*
 671 *Bioinform* 2005;2:330–8.
- [24] Jain S, Bader GD. An improved method for scoring
 673 protein-protein interactions using semantic similarity within
 674 the gene ontology. *BMC Bioinformatics* 2010;11:562.
- [25] Guo X, Shriver CD, Hu H, Liebman MN. Analysis of metabolic
 676 and regulatory pathways through Gene Ontology-derived
 677 semantic similarity measures. *AMIA Annu Symp Proc* 2005:972. 678

- 679 [26] Tedder PM, Bradford JR, Needham CJ, McConkey GA, Bulpitt
680 AJ, Westhead DR. Gene function prediction using semantic
681 similarity clustering and enrichment analysis in the malaria
682 parasite *Plasmodium falciparum*. *Bioinformatics* 2010;26:
683 2431-7.
- 684 [27] Wang JZ, Du Z, Payattakool R, Yu PS, Chen CF. A new method
685 to measure the semantic similarity of GO terms.
686 *Bioinformatics* 2007;23:1274-81.
- 687 [28] Wolfel T, Hauer M, Klehmann E, Brichard V, Ackermann B,
688 Knuth A, et al. Analysis of antigens recognized on human
689 melanoma cells by A2-restricted cytolytic T lymphocytes
690 (CTL). *Int J Cancer* 1993;55:237-44.
- 691 [29] Hohaus A, Person V, Behlke J, Schaper J, Morano I, Haase H.
692 The carboxyl-terminal region of ahn provides a link
693 between cardiac L-type Ca²⁺ channels and the actin-based
694 cytoskeleton. *FASEB J* 2002;16:1205-16.
- 695 [30] Paul AS, Pollard TD. Review of the mechanism of processive
696 actin filament elongation by formins. *Cell Motil Cytoskeleton*
697 2009;66:606-17.
- 698 [31] Han JD, Bertin N, Hao T, Goldberg DS, Berriz GF, Zhang LV,
699 et al. Evidence for dynamically organized modularity in the
700 yeast protein-protein interaction network. *Nature* 2004;430:
701 88-93.
- 702 [32] Bassel GW, Lan H, Glaab E, Gibbs DJ, Gerjets T, Krasnogor N,
703 et al. Genome-wide network model capturing seed
704 germination reveals coordinated regulation of plant cellular
705 phase transitions. *Proc Natl Acad Sci U S A* 2011;108:9709-14.
- 706 [33] Ogata Y, Chikayama E, Morioka Y, Everroad RC, Shino A,
707 Matsushima A, et al. ECOMICS: a web-based toolkit for
708 investigating the biomolecular web in ecosystems using a
709 trans-omics approach. *PLoS One* 2012;7:e30263.
- 710 [34] Higashi T, Ikeda T, Murakami T, Shirakawa R, Kawato M,
711 Okawa K, et al. Flightless-I (Fli-I) regulates the actin assembly
712 activity of diaphanous-related formins (DRFs) Daam1 and
713 mDia1 in cooperation with active Rho GTPase. *J Biol Chem*
714 2010;285:16231-8.
- 715 [35] Matza D, Badou A, Kobayashi KS, Goldsmith-Pestana K,
716 Masuda Y, Komuro A, et al. A scaffold protein, AHNK1, is
717 required for calcium signaling during T cell activation.
718 *Immunity* 2008;28:64-74.
- 719 [36] Borgonovo B, Cocucci E, Racchetti G, Podini P, Bachi A,
720 Meldolesi J. Regulated exocytosis: a novel, widely expressed
721 system. *Nat Cell Biol* 2002;4:955-62.
- 722 [37] Matza D, Badou A, Jha MK, Willinger T, Antov A, Sanjabi S,
723 et al. Requirement for AHNK1-mediated calcium signaling
724 during T lymphocyte cytolysis. *Proc Natl Acad Sci U S A*
725 2009;106:9785-90.
- 726 [38] Mersich AT, Miller MR, Chkourko H, Blystone SD. The formin
727 FRL1 (FMNL1) is an essential component of macrophage
728 podosomes. *Cytoskeleton (Hoboken)* 2010;67:573-85.
- 729 [39] Vogt DL, Gray CD, Young III WS, Orellana SA, Malouf AT.
730 ARHGAP4 is a novel RhoGAP that mediates inhibition of cell
731 motility and axon outgrowth. *Mol Cell Neurosci* 2007;36:
732 332-42.
- 733 [40] Fujimoto M, Imai K, Hirata K, Kashiwagi R, Morinishi Y,
734 Kitazawa K, et al. Immunological profile in a family with
735 nephrogenic diabetes insipidus with a novel 11 kb deletion in
736 AVPR2 and ARHGAP4 genes. *BMC Med Genet* 2008;9:42.
- 737 [41] Foletta VC, Brown FD, Young III WS. Cloning of rat
738 ARHGAP4/C1, a RhoGAP family member expressed in the
739 nervous system that colocalizes with the Golgi complex and
740 microtubules. *Brain Res Mol Brain Res* 2002;107:65-79.
- 741 [42] Wells CD, Fawcett JP, Traweger A, Yamanaka Y, Goudreault
742 M, Elder K, et al. A Rich1/Amot complex regulates the Cdc42
743 GTPase and apical-polarity proteins in epithelial cells. *Cell*
744 2006;125:535-48.
- 745 [43] Harada A, Furuta B, Takeuchi K, Itakura M, Takahashi M,
746 Umeda M. Nadrin, a novel neuron-specific GTPase-activating
747 protein involved in regulated exocytosis. *J Biol Chem*
748 2000;275:36885-91.
- 749 [44] Richnau N, Aspenstrom P. Rich, a rho GTPase-activating
750 protein domain-containing protein involved in signaling by
751 Cdc42 and Rac1. *J Biol Chem* 2001;276:35060-70.
- 752 [45] Yi C, Troutman S, Fera D, Stemmer-Rachamimov A, Avila JL,
753 Christian N, et al. A tight junction-associated
754 Merlin-angiomin complex mediates Merlin's regulation of
755 mitogenic signaling and tumor suppressive functions. *Cancer*
756 *Cell* 2011;19:527-40.
- 757 [46] Yu G, Wang LG, Han Y, He QY. clusterProfiler: an R package
758 for comparing biological themes among gene clusters. *Omic*
759 2012;16:284-7.
- 760 [47] Haase H. Ahnak, a new player in beta-adrenergic regulation
761 of the cardiac L-type Ca²⁺ channel. *Cardiovasc Res* 2007;73:
762 19-25.
- 763 [48] Haase H, Alvarez J, Petzhold D, Doller A, Behlke J, Erdmann J,
764 et al. Ahnak is critical for cardiac Ca (V) 1.2 calcium channel
765 function and its beta-adrenergic regulation. *FASEB J* 2005;19:
766 1969-77.
- 767 [49] Dempsey BR, Rezvanpour A, Lee TW, Barber KR, Junop MS,
768 Shaw GS. Structure of an asymmetric ternary protein
769 complex provides insight for membrane interaction.
770 *Structure* 2012.
- 771 [50] Rezvanpour A, Santamaria-Kisiel L, Shaw GS. The
772 S100A10-annexin A2 complex provides a novel asymmetric
773 platform for membrane repair. *J Biol Chem* 2011;286:
774 40174-83.
- 775 [51] Huang Y, Laval SH, van Remoortere A, Baudier J, Benaud C,
776 Anderson LV, et al. AHNK, a novel component of the
777 dysferlin protein complex, redistributes to the cytoplasm
778 with dysferlin during skeletal muscle regeneration. *FASEB J*
779 2007;21:732-42.
- 780 [52] Szabadkai G, Bianchi K, Varnai P, De Stefani D, Wieckowski
781 MR, Cavagna D, et al. Chaperone-mediated coupling of
782 endoplasmic reticulum and mitochondrial Ca²⁺ channels. *J*
783 *Cell Biol* 2006;175:901-11.
- 784 [53] Macer DR, Koch GL. Identification of a set of calcium-binding
785 proteins in reticuloplasm, the luminal content of the
786 endoplasmic reticulum. *J Cell Sci* 1988;91(Pt 1):61-70.
- 787 [54] Zheng Z, Venkatapathy S, Rao G, Harrington CA. Expression
788 profiling of B cell chronic lymphocytic leukemia suggests
789 deficient CD1-mediated immunity, polarized cytokine
790 response, altered adhesion and increased intracellular
791 protein transport and processing of leukemic cells. *Leukemia*
792 2002;16:2429-37.
- 793
- 794